Eleventh International Conference on the Bearing Capacity of Roads, Railways and Airfields, Volume 3 – Hoff, Mork & Saba (eds)

Assessment of construction and demolition waste materials for sublayers of low traffic rural roads

S. Pourkhorshidi & C. Sangiorgi
Department of Civil, Chemical, Environmental, and Materials Engineering (DICAM), University of Bolognas, Bologna, Italy

D. Torreggiani & P. Tassinari
Department of Agricultural and Food Sciences (DISTAL), University of Bologna, Bologna, Italy

ABSTRACT: The need for exploiting massive amounts of natural raw materials for constructing pavements of roads as a key element for development of infrastructures in modern age, together with enormous production amounts of wastes related to civil engineering activities as biggest portion of solid waste generated all over the world, have highlighted the importance of utilizing recycled aggregates of these materials in road pavement layers. The key factor in this quest, is to evaluate load-bearing abilities of various kinds of waste aggregates. Aggregates of reclaimed asphalt, pre-stressed or normal concrete, masonry and demolition waste (CDW) exhibit different behavior under loading after compaction. The ideal situation would be to achieve the densest compacted and durable layer in order to get the highest durability, comparing to traditional road materials. In this study, aggregates from four types of recycled materials are being subjected to study for unbound and cemented pavement layers. Initial laboratory evaluations of size and composition are followed by constructing a field on a subgrade with high non-homogenous surface. Vibrating elastic modulus (E_{vib}) for these materials were determined by Continuous Compaction Control (CCC) Oscillating Rollers. It is observed that, despite the weaknesses arisen from weak components such as masonry and elongated tiles, the stabilized distribution of the particle size can accelerate reaching to final compaction of unbound aggregates with roller passing. This process could be repeated with more or less same pattern in cemented layer, which exhibited an enhanced stiffness and uniformity in order to minimize the weak parts of non-uniform subgrade layer, and provide a high rigid pavement.

Keywords: construction and demolition waste, recycling, continuous compaction control, foundation layers, cemented layers

1 INTRODUCTION

By developing new innovative technologies for road construction in recent years, rollers with continuous compaction control (CCC) capability are more and more utilized for constructing the various layers of pavements. Achieving high efficiency of compaction by these rollers has been a key topic for many researches. Most roller manufacturers follow the corresponding line of evaluating how the soil under compaction reacts to the roller and use this measurement to determine parameters referable to bearing capacity (Dondi et al. 2014).

DOI: 10.1201/9781003222910-50

On the other hand, the need for providing raw materials for pavements is soared in recent decades due to huge amount of road construction all over the world, especially in developing countries, owing to facilitated technological possibilities and solutions. Considering large values of waste materials obtained from civil engineering activities, environmental, sustainability and economic considerations strongly suggest applying recycled construction and demolition waste materials as a substitute of virgin raw materials (Pourkhorshidi et al. 2020, Kovanda 2020, Tansel 2020).

The importance of rural roads in stimulating both economic growth and social development has been observed in many researches (Plessis-Fraissard 2007). The necessity for constructing rural road networks with the most cheap, durable and reliable possible methods with available materials, featured the study of unbound and cement-bound pavements to be used in the rural low-traffic pavements (Del Rey et al. 2016)

Researches on utilizing the recycled solid waste materials of construction and demolition in various layers of road pavements are vastly done all over the world (Barbudo et al. 2012, Gómez-Meijide & Pérez 2014, B. Gómez-Meijide et al. 2016); however, a limited number of them studied using continuous compaction control on recycled materials (Vennapusa et al. 2010). Sangiorgi et al. showed that construction and demolition material (CDW), laid using the same compaction process, could contribute differently to the bearing capacity of a double-layered embankment. Using CCC as an efficient method, they demonstrated that CCC measured E_{vib} moduli increase significantly as CDW compaction progresses. As the number of passes increases, the rate at which stiffness increases diminishes, and there is greater variability in stiffness for each kind of recycled material. Also, Light Weight Deflectometry (LWD) were found to correlate well despite different recorded value sizes for the moduli (Sangiorgi et al. 2015). In another study by Sangiorgi et al., it was concluded that CCC measured moduli shown significant increase with the progress of CDW compaction, even with values being highly affected by the presence of a layered structure and a weak subgrade. Also, the so-called Compaction Paths, starting from loose material values, show different trends of stiffnesses for different layers and materials. LWD measurements were very well correlated comparing to E_{vib} data. They proved that coupling CCC rollers and LWDs' measurements for the evaluation of earthworks should require a minimum CCC- measured value for given compaction amplitude (Sangiorgi et al. 2012).

In this research, an attempt is made to study the evaluation of stiffness by vibratory roller passes on four different recycled materials in unbound conditions, and also to see the stiffness gain in their cement-bound state.

2 MATERIALS

In total, five types of recycled materials obtained from civil engineering activities processed in an Italian high-quality recycling plant near the city of Imola offering licensed recycled aggregates for construction purposes, were utilized for constructing the unbound and cement-bound layers of a trial pavement. All the materials have European certificates and are in the range of 0-30mm size. Three out of five, have stabilized dense gradation envelopes, which make them suitable for being used in pavement applications. The amount of their floating elements is small. The compositions of these materials are listed in Table 1, and their particle size distributions are shown together with the size envelope of Italian authorities for road pavement materials in Figure 1. More technical properties of the materials are given in Table 2.

3 TRIAL FIELD AND COMPACTING METHOD

An experimental site was made in the mentioned recycling plant in Imola, Italy, in a location where high number of heavy trucks pass every working day (at least 5 to 10 heavy lorries each day). The subgrade of the site was constructed in the previous years with very thick

Table 1. Characteristics of the used recycled materials.

Material	Abbreviation	Containing	Composition
Stabilized mix of Crushed concrete and Reclaimed asphalt	ASFC	- Concrete-based building demolition rubble: industrial floors, beams, pillars, etc. - Vineyard poles in reinforced concrete - Asphalt slabs and Reclaimed asphalt pavement	- 50% concrete - 50% RAP
Construction and Demolition waste	CDW	- "Mixed" building demolition rubble not differentiated: brick, concrete, plaster, sand, cement, ceramic, etc. - Ceramic Tiles (ceramic industry waste) - Industrial waste (steel/foundry slag, sandblasting dust)	- 50% demolition mix - 20% ceramic waste - 30% industrial waste
Stabilized Recycled concrete	RCA	- Concrete-based building demolition rubble: industrial floors, beams, pillars, concrete tiles, etc. - Reinforced concrete of Vineyard poles	- 100% concrete rubble
Stabilized Crushed concrete sleepers	TRV	-Reinforced concrete of railway sleepers	- 100% concrete rubble from sleepers
Mix of Crushed sleepers and foundry waste	MTRV	- Reinforced concrete of railway sleepers - Industrial waste (steel/foundry slag, sandblasting dust)	- 60% concrete rubble from sleepers - 40% industrial waste

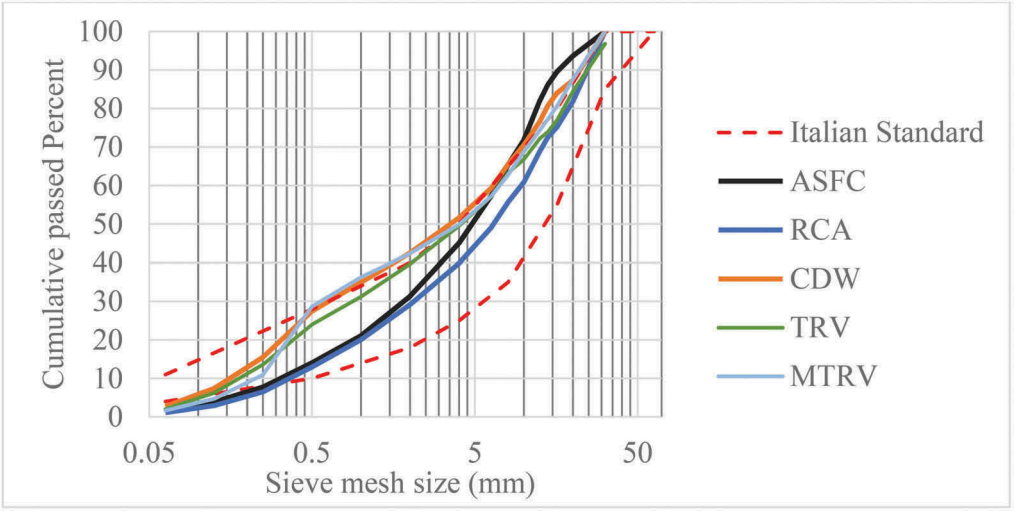

Figure 1. Particle size distribution of recycled materials.

layers of CDW and hardened by passing numerous vehicles including dozers and excavators. Four different layers were identified by means of a specific trench dug to the depth of 1.2 meters (Figure 2). Subgrade was placed in the past as a heterogeneous filling blend of CDW, clayey soil and other waste materials, compacted in several years by the plant traffic. The subgrade surface was roller-compacted and proven in 4 lanes before laying the first layer of new materials.

Table 2. Properties of recycled materials.

Material	Optimum moisture content (%)	MDD (kg/dm^3)	Un-soaked California bearing ratio (%)	Soaked California bearing ratio (%)	Los Angeles index (%)
ASFC	6.27	1.96	92	50	24
RCA	10.80	1.92	165	151	31
CDW	9.55	1.94	159	122	37
TRV	10.85	2.00	202	295	29
MTRV	10.79	1.94	110	150	30

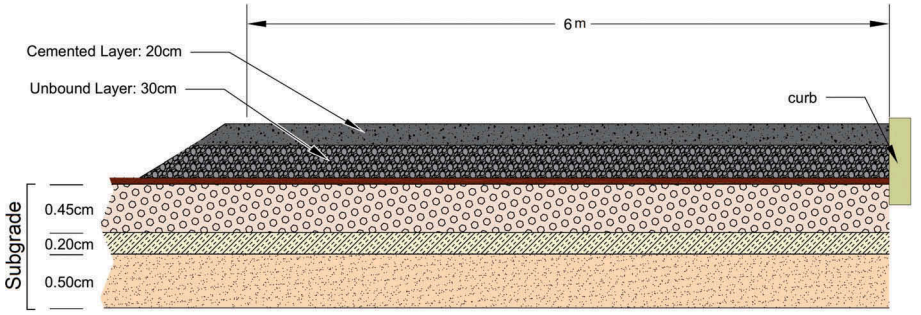

Figure 2. Schematic cross-section of subgrade, unbound and cement-bound layer.

An area 6 meters wide and 36 meters long was chosen for constructing the road and laying the selected recycled materials. The aerial image of the site is shown in Figure 3.

Figure 3. Schematic plan of constructed road and compaction lanes, Left: Sections of unbound materials and three lanes of roller compaction, Right: Cemented layers and lanes.

For target thickness of 30 cm considered for unbound base layer, about 35 cm depth of four type of materials was laid and leveled in the area each for each section length of 9 meters, after aggregates being hauled by loaders. After leveling by grader, the layer was compacted in three lanes by a heavy CCC roller setting a constant vibration amplitude. The subgrade and unbound base layer compaction and test processes were performed by means of a BOMAG

BW219 DH-5 compactor with a drum width of 212cm. Also, the speed and frequency of the roller compactor were controlled and fixed in order to maintain a comparable rolling condition for all three lanes. One each lane, 4 sets of forward vibrating and reverse static compaction were done and the stiffness data were collected.

For the Cement-bound layer, two materials of ASFC (mix of crushed concrete and reclaimed asphalt) and MTRV (mix of crushed sleepers and foundry waste) were selected to be mixed with cement and water, for a target layer of 20 cm thickness. 3% Portland cement was added to the two recycled materials of ASFC and MTRV with an automatic BLEND E050 blending machine, with the capacity of $14m^3$ of cemented mix ($10m^3$ aggregate and 4 m^3 cement). The measured humidity of the mixes were 7.4% and 4.5% for ASFC and MTRV, respectively.

Two cemented materials were laid in parallel as shown in Figure 3, each layer had a width of 3 meters in order to create 8 different layered pavements in the trial site. One lane of vibrating compaction per each cement-bounded material was done by a BOMAG BW174AP-4V AM roller in order to compact and simultaneously evaluate the vibratory stiffness. A Lightweight deflectometry (LWD) was done in between the passes over the cemented material by mean of a ZORN ZFG2000 portable deflectometer.

The specifications of compacting rollers are reported in Table 3.

Table 3. Specifications of roller compactors.

	Subgrade and Unbound Base layer	Cement-bound layer
Model	BOMAG BW219 DH-5	BOMAG BW174AP-4 VAM
Mass	19400 kg	9500 kg
Drum width	212 cm	170 cm
Linear load	60.1 kg/cm	29.8 kg/cm
Roller speed (average)	3.7 km/h	2.4 km/h
Vibration frequency	24 Hz	45 Hz
Manual Amplitude	1.2 mm	0.8 mm

4 RESULTS AND DISCUSSION

The output of the rollers included E_{vib} graphs plot versus the longitudinal position of the roller compactor. The triggering of the data acquisition system was done manually at each forward pass. Data were saved in the cloud and printed on paper for further analysis. Matching of start-end points was made by means of reference points.

4.1 *Stiffness variation*

The E_{vib} values of the subgrade lanes are shown in Figure 4. The dashed lines show the adjacent sections of the subsequent unbound layer which would be layered in next stage. It is shown that despite revealing an inhomogeneity, stiffness modulus of all lanes follow similar patterns all over the length of the field. At a distance of 14 meters, there was a pipe passing under the subgrade which caused the weakness clearly visible by decrease in the E_{vib} values. The first lane had a lower E_{vib} graph which could be due to proximity to the concrete curb, from which trucks are usually distant for maneuvering. The overall width of subgrade is less than four lanes done with roller drum width of 212 cm, so the drum accelerometer sensor of roller which is located in one side of the drum, had fallen over previously roller-proven lane. Among the sections considered for the next layer of unbound materials, it is more or less obvious that section 2 has the lowest stiffness, while there is a peak in the border of sections 2 and 3.

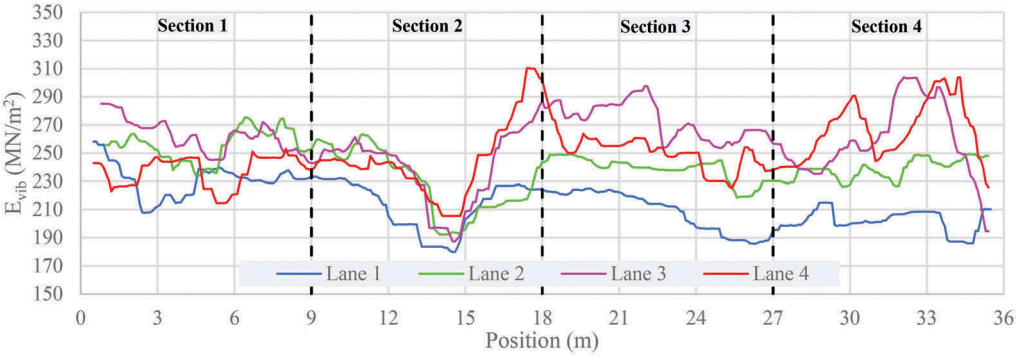

Figure 4. Vibratory modulus of subgrade (4 parallel overlapping lanes).

By constructing the new unbound base layer, another set of E_{vib} data was recorded for three new compaction lanes: east (close to curb), mid and west (the lane with free embankment). These data are shown in the graphs of Figure 5. There are some common details in all three graphs. First, all graphs follow the same pattern comparatively, considering subgrade stiffness inhomogeneity and diversity in materials of sections. For example, the location of weak stiffness regarding to weakness of subgrade under the pipe is obvious in all graphs, in spite of becoming less distinct in the west lane which is far from the curb. Secondly, the value of overall E_{vib} increase by the number of rollers passes. The E_{vib} increasing in various sections are noticeably different. In CDW, the E_{vib} graphs are closer to each other pass 1 to 4, but for other materials, especially RCA, the increase in E_{vib} is clearly visible. This could be related to many factors including the composition of mix constituents and their resistance to fragmentation. For materials with larger quantities of cementitious particles, the resistance to breaking under compaction is higher than CDW which has mainly masonry and bricks particles.

Yellow dashed lines shown the average E_{vib} value of the last pass in each section of material. It is seen that the order of E_{vib} value in the three section of CDW, RCA and ASFC is more or less the same for all lanes: CDW has the lowest value and ASFC has the relatively high average E_{vib} value. The section of TRV show a different behavior in east and west lanes which could be due to the free end edges of the embankment and the effect of subgrade stiffness variations. The relative values of final pass vibration stiffness of each section are not completely in agreement with the materials properties of each sections, which for some CDWs are relatively low (Poon & Chan 2006).

In the east lane, the drastic variations of E_{vib} are seen in first pass, which change to smoother peaks in the last pass (pass 4). However, despite a similar trend is repeated in E_{vib} of west lane, but some new peaks appear by increasing the number of passes. This proves the fact that, at least two different mechanisms contribute to the recorded E_{vib} value: first, the trace of varying stiffness of bottom layers (here: subgrade) on the upper layers, and secondly, the zonal high-compacted small segments created in last passes due to geometrical inhomogeneities in distribution of material layering and leveling.

The E_{vib} graphs of cemented layers are shown in Figure 6. As the material under compaction is unique all over the lane length, any change in the E_{vib} graph along the lane could be explained as the imprint of the base compacted layer on the superimposed cement-bounded layer.

However, the variation of E_{vib} plots in the cement-bound material over the length of the lane are much less than the variations in the unbound base layer, and cemented layers are more homogenous in terms of stiffness. The average value of E_{vib} for the last pass in all the sections (orange dashed lines) are more or less in the same range. This could be described as the positive outcome of well compacted base on the next layer, which provided a more uniform stiffness all over the lane. This homogeneity of stiffness is more evident in cemented MTRV than ASFC.

At the end of the base layer compaction, the mean E_{vib} values increase of approximately 20% with respect to pass 1 which was done over fresh material; it can be stated that each pass

of vibratory compaction increased the E_{vib} of 5%, on average. In studying the CCC method, the achievement of maximum compaction is controlled through the percentage difference between the measured values (MVs) of two consecutive passes: compaction must be continued until the mean roller MV is less than 5% greater than the mean value from the previous pass. For small sites, this guarantees that no further compaction is possible and that if the weak spot tests are positive, than all the area has, on average, sufficient bearing capacity (Sangiorgi et al. 2012). Based on this, it is possible to infer that by only considering above mentioned 5% increment limit rule for the unbound layer, even one pass with the considered energy (frequency and amplitude) appears to be enough, which does not look to be cogent. So, in case of recycled materials, additional tests and methods will be necessary to support the sufficiency of vibratory roller passes for compacting the unbound layer. This is because their stiffness increments could be not fallen in a minimum range by escalating pass number, and persist in later passes.

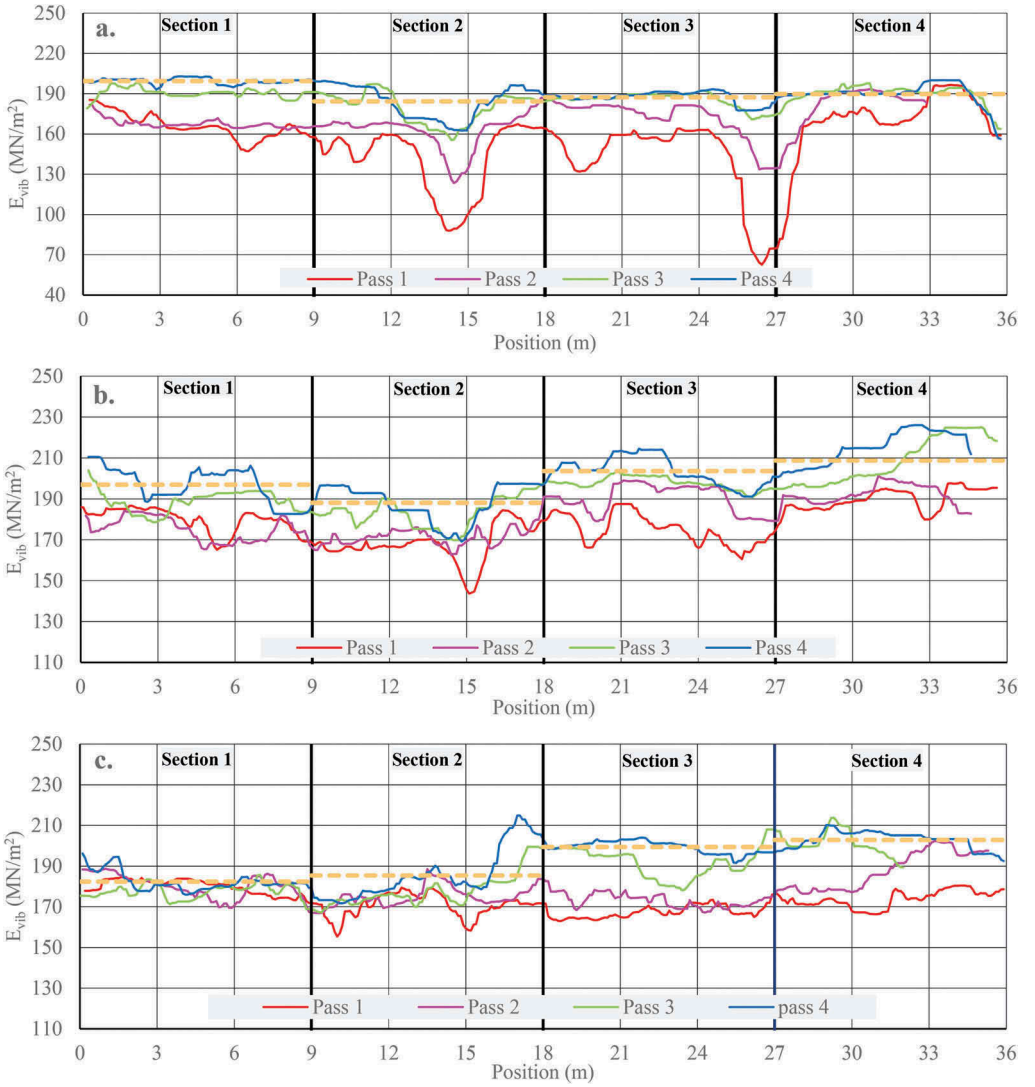

Figure 5. E_{vib} modulus of unbound base layer: a) East Lane, b) Middle Lane, c) West Lane, Section 1: ASFC, Section 2: RCA, Section 3: CDW and Section 4: TRV.

For cement-bound layer, alternatively, the distribution of E_{vib} graph increments is not uniform between passes. It is obvious that in cement-bound layers, the last passes have very close E_{vib} and graphs of final passes become more entangled. Considering that the total number of passes for cement-bound layer is 6, which is more than the passes of unbound layer (4 passes), it seems unlike unbound layer, there would be no increase in E_{vib} graphs of cement-bounded layer by any further extra passes of roller. This could be due to the fact that cement-bounded materials reach their final compaction limit in specified roller vibration energy (related to vibration frequency and amplitude) after third pass. The LWD evaluation between each pass (section 4.3) confirms this.

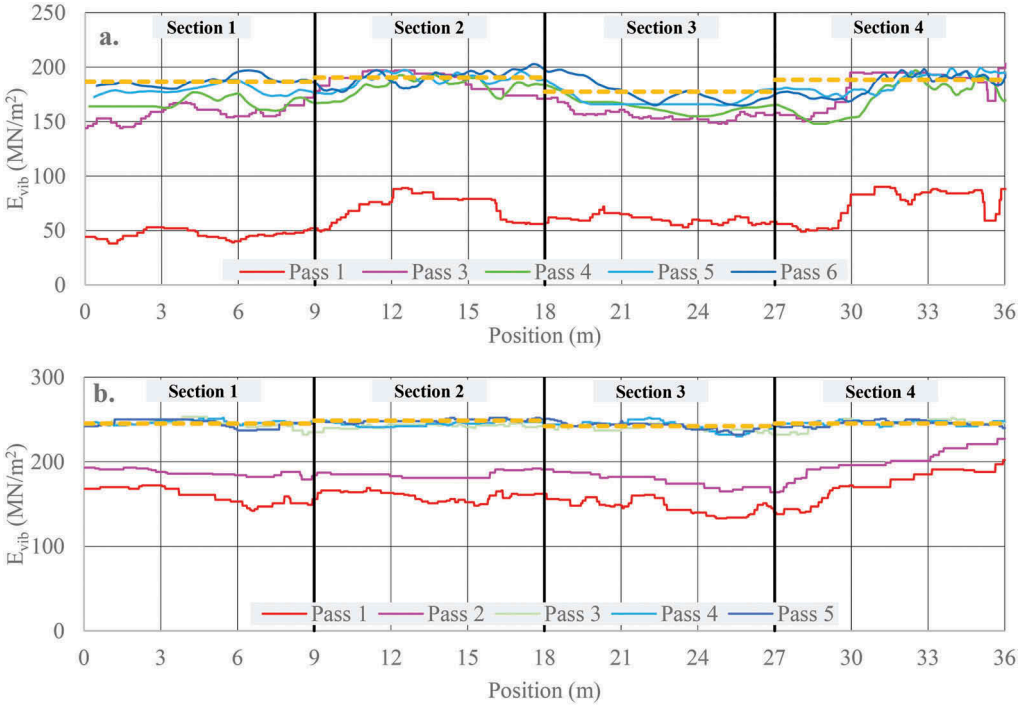

Figure 6. E_{vib} stiffness modulus in the cement-bound layer: a) Lane 1 - Cemented ASFC; b) Lane 2: Cemented MTRV.

4.2 *Analysis of compaction development*

The evolution of stiffness increase by the number of passes in unbound layer, can be represented in an E_{vib} pass "i" - E_{vib} pass "i+1" graph where the 45° line represents the values of equality between two subsequent vibratory passes, thus meaning that on the diagonal line no increase in stiffness has occurred. The clouds of points tend to get close to the 45° line as compaction progresses. Points below the line represent field positions where E_{vib} reduces from pass "i" to pass "i+1". This graph shown in Figure 7, where the overall progress can be traced by joining the mean values point of each couple of consecutive passes on the E_{vib} pass "i" - E_{vib} pass "i+1" plane.

This method represents no significant variation in the rate of change between the passes in unbound conditions, which could be in contrast with what could be visually seen in E_{vib} graphs of three roller compaction lanes for all sections. This dissimilarity proves the need for studying details of the stiffness gaining mechanisms in different recycled materials. The separation of different sections data clouds could prove how different materials exhibit different compaction patterns under the vibration of roller in various consecutive passes. An intuitive

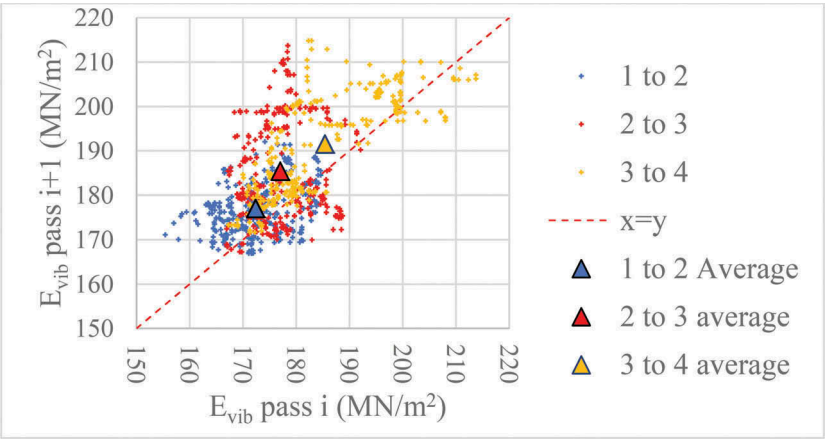

Figure 7. Stiffness values of unbound base layer in pairs of consecutive passes in all sections.

demonstration of the evolution of the stiffness could be given with the Compaction Paths (CP) polyline on each field, as shown in Figure 8.

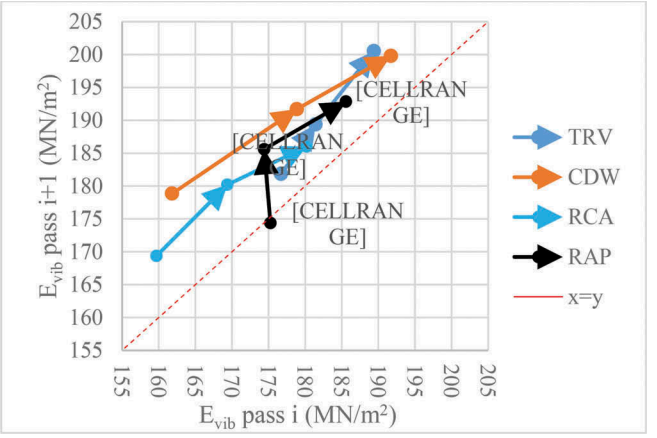

Figure 8. Compaction paths of different materials of unbound base layer.

As it is shown in Figure 8, the changing in stiffness of different materials by applying vibratory pass vary from one recycled material to the another. Considering Compaction path graphs, highest evolution in stiffness by roller compaction happens in CDW (with E_{vib} increase about 25%) and crushed sleepers (with E_{vib} increase of 15%)

The stiffness graphs in CDW became closer to each other in the last passes (3 to 4) than in initial passes (1 to 2). A possible explanation could be due to the type of substances and their portions, which are the only major dissimilarity among the different materials used in this study. CDW contains masonry and brittle tiles which fragmentation under compaction could change their particle size distribution and by increasing the number of passes, vibration could cause rearranging the broken fine particles as the compaction proceeds. This trend is also seen, but to a lower extent, in the RCA. However, in ASFC containing bituminous particles, the behavior is different, while the steps of E_{vib} increment increase in second to third pass and decrease in last ones (3 to 4), and for TRV containing high strength concrete aggregates the increment of stiffness increase pass after pass, making their stiffness development point higher the than 45° line. One possible explanation for extraordinary behavior of ASFC is presence of

two processes working in opposite directions: Bituminous particles of ASFC are less brittle than other components (low Los Angeles test index of ASFC proves this) and they can also damp the energy of vibration due to their visco-elastic nature. This feature can cause the displacement of the aggregates under vibratory compaction in initial passes. This loosening effect can be compensated by the mechanism of filling voids between the aggregates by finer broken aggregates (of other brittle components, such as cemented particles). This improves the compaction degree, diminish the stiffness increment in the last passes and makes the compaction path converge to 45° line.

In crushed sleepers, due to the high strength of source pre-stressed concrete used for manufacturing the railway sleepers, the energy of vibrating compaction roller could not be enough for smashing all coarse aggregates and only minor change in size distribution would happen. This can be followed by eased particle displacement and the process continues in next passes as most coarse aggregates remain, which causes the material gain stiffness by each pass.

4.3 *Light weight deflectometry*

The evolution of the stiffness of cement-bound layer by the passes measured by LWD point test is shown in Figure 9. It is evident that there is an optimum number of passes for cement-bound layers in order to reach their highest stiffness by vibratory roller compaction. This graph is in agreement with the E_{vib} graphs, where the last passes of the cement-bound layer are very close to each other, and they do not show any extra increment in stiffness by further passes. It is seen that ASFC achieves stiffness by less passes than MTRV in cement-bound layers. Moreover, the rate of reaching the final stiffness from first pass in ASFC is almost twice the one for mixed crushed sleepers. These observations could be an indication of the fact that the compaction energy needed for reaching an optimal compaction in recycled materials with hard high-strength components are higher than those with weaker aggregates.

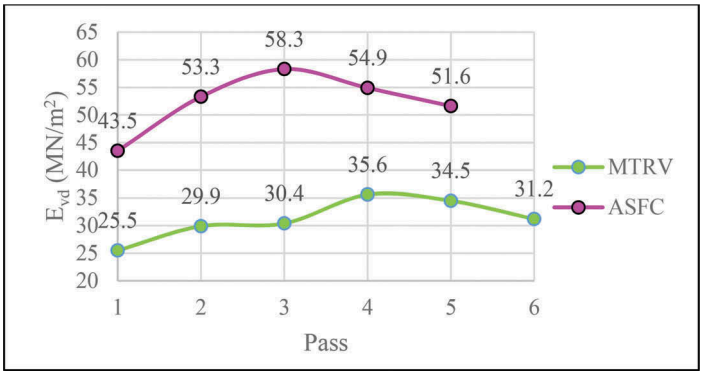

Figure 9. Lightweight Deflectometry test (LWD) results after each roller pass over cement-bound layers.

5 CONCLUSIONS

In this research, five types of recycled aggregates from waste of civil engineering activities were utilized for constructing unbound and cement-bound layers for low traffic roads by using vibratory compaction roller and their embedded CCC systems. The following outcomes can be concluded:

- Different recycled materials exhibit similar behavior with different extent in vibrating roller compaction. Recycled materials with weak components -like masonry and brick aggregates in CDW- could gain stiffness in initial passes due to the fragmentation and change in

aggregate size distribution, however, harder constituents like crushed high-strength concrete aggregates in crushed sleepers cause persisting the stiffness increase rate of the material until later passes of vibrating roller.
- Relying only on the CCC studies could not be sufficient for determining the number of necessary passes for all kinds of recycled material, as even first passes could appear to meet the rule of 5% increment. Therefore, supplementary tests and methods could be required to identify the number of vibratory roller passes for compacting the unbound layer.
- Compaction path shows the change in stiffness of different materials by applying consecutive vibratory passes. These paths vary from one recycled material to the other. CDW and ASFC show highest and lowest stiffness gains by consecutive passes, relatively. This could be due to different strength and brittleness of their constituents.
- Lightweight deflectometry test (LWD) suggests what was visible by E_{vib} records on cement-bound layers: there is an optimum number of passes for cement-bound material to gain stiffness during compaction. Extra passes will not increase the E_{vib} of the compacted material. This number could be different for various materials.

ACKNOWLEDGMENT

The authors acknowledge the Italian companies of C.A.R Inerti srl and BOMAG Italia srl for providing materials, technicians and necessary machinery for experimental field operations of this research.

REFERENCES

A. Barbudo, F. Agrela, J. Ayuso, J.R. Jiménez, C.S. Poon, 2012 *Statistical analysis of recycled aggregates derived from different sources for sub-base applications*. Constr. Build. Mater. 28, 129–138. https://doi.org/10.1016/j.conbuildmat.2011.07.035.

I. Del Rey, J. Ayuso, A. Galvín, J. Jiménez, A. Barbudo, 2016 *Feasibility of Using Unbound Mixed Recycled Aggregates from CDW over Expansive Clay Subgrade in Unpaved Rural Roads*, Materials (Basel). 9, 931. https://doi.org/10.3390/ma9110931.

G. Dondi, C. Sangiorgi, C. Lantieri, 2014 *Applying Geostatistics to Continuous Compaction Control of Construction and Demolition Materials for Road Embankments*. J. Geotech. Geoenvironmental Eng. 140, 06013005. https://doi.org/10.1061/(asce)gt.1943-5606.0001044.

B. Gómez-Meijide, I. Pérez, A.R. Pasandín, 2016 *Recycled construction and demolition waste in Cold Asphalt Mixtures: Evolutionary properties*. J. Clean. Prod. 112, 588–598. https://doi.org/10.1016/j.jclepro.2015.08.038.

J. Kovanda, 2020 *Raw material consumption or total material consumption? Which indicator is better for evaluating material resource consumption and environmental pressure?*. Environ. Monit. Assess. 192. https://doi.org/10.1007/s10661-020-08343-w.

M. Plessis-Fraissard, 2007 *Planning roads for rural communities*, Transp. Res. Rec. 1, 1–8. https://doi.org/10.3141/1989-01.

C. Poon, D. Chan, 2006 *Feasible use of recycled concrete aggregates and crushed clay brick as unbound road sub-base*, Constr. Build. Mater. 20, 578–585.

C. Sangiorgi, C. Lantieri, G. Dondi, 2015 *Construction and demolition waste recycling: An application for road construction*. Int. J. Pavement Eng. 16, 530–537. https://doi.org/10.1080/10298436.2014.943134.

C. Sangiorgi, A. Marradi, H. Kloubert, W. Wallrath, 2012 *A ccc experimental site for studying the compaction evolution of C&D materials*. in: Proc. 3rd Int. Semin. Earthworks Eur. Col. FGSV Verlag GmbH, COLOGNE, pp. 115–126.

B. Tansel, 2020 *Increasing gaps between materials demand and materials recycling rates: A historical perspective for evolution of consumer products and waste quantities*, J. Environ. Manage. 276, 111196. https://doi.org/10.1016/j.jenvman.2020.111196.

P.K.R. Vennapusa, D.J. White, M.D. Morris, 2010 *Geostatistical Analysis for Spatially Referenced Roller-Integrated Compaction Measurements*, J. Geotech. Geoenvironmental Eng. 136, 813–822. https://doi.org/10.1061/(asce)gt.1943-5606.0000285.